Optimization of dry etching parameters for fabrication of polysilicon waveguides with smooth sidewall using a capacitively coupled plasma reactor

Surya Cheemalapati, Mikhail Ladanov, John Winskas, and Anna Pyayt*

Department of Chemical and Biomedical Engineering, University of South Florida,
4202 E. Fowler Ave. ENB118, Tampa, Florida 33620, USA

*Corresponding author: pyayt@usf.edu

Received 9 May 2014; revised 28 June 2014; accepted 22 July 2014;
posted 1 August 2014 (Doc. ID 211810); published 28 August 2014

In this paper, we demonstrate the optimization of a capacitively coupled plasma etching for the fabrication of a polysilicon waveguide with smooth sidewalls and low optical loss. A detailed experimental study on the influences of RF plasma power and chamber pressure on the roughness of the sidewalls of waveguides was conducted and waveguides were characterized using a scanning electron microscope. It was demonstrated that optimal combination of pressure (30 mTorr) and power (150 W) resulted in the smoothest sidewalls. The optical losses of the optimized waveguide were 4.1 ± 0.6 dB/cm.
© 2014 Optical Society of America
OCIS codes: (230.7370) Waveguides; (240.5770) Roughness; (220.4000) Microstructure fabrication.
http://dx.doi.org/10.1364/AO.53.005745

1. Introduction

Optical waveguides are critical building blocks of on-chip photonics. Quality of an optical waveguide is largely defined by its optical loss. For straight polysilicon waveguides, absorption and scattering at grain boundaries [1,2], substrate coupling, and radiation loss at etched waveguide sidewalls are the main sources of optical loss [3–5]. Therefore, thicker waveguide claddings can be used to minimize substrate coupling loss and fabrication can be optimized to decrease the surface roughness [1,6,7]. A photolithographic mask used for waveguide patterning has to be printed with high resolution to reduce line edge roughness [8,9]. Additionally, postprocessing methods can be used to make sidewalls smoother. They include gas phase oxidation [10], wet chemical oxidation [11], hydrogenation [2], resist reflow [12], end facet polishing [13], and related processes [14]. This requires the introduction of additional fabrication steps, and increases error rates and cost of the fabrication process. Ideally, fabrication should be done using a simple process with a small number of steps. Since etching of the waveguide is frequently done using one of the dry etching techniques, and capacitively coupled plasma reactors are still widely spread, we conducted a study of optimization of the optical waveguide fabrication using this equipment.

Traditionally, etching of planar waveguides is done using either inductively coupled plasma (ICP) with a passivation gas flow or electron cyclotron resonance (ECR) plasma [15–17], since they have a high density of plasma, high directionality, and higher power levels. However, this equipment is very expensive and, thus, unavailable in many microfabrication facilities, while capacitively coupled plasma reactors are less expensive and more readily available, but were not previously used for this application [18]. Here, we demonstrate the application of a capacitively coupled plasma reactor for the fabrication of polysilicon photonic waveguides with a low loss of 4.1 ± 0.6 dB/cm by the optimization of process parameters, such

1559-128X/14/255745-05$15.00/0
© 2014 Optical Society of America

as pressure and power using a careful design of experiments, and observe a 62% improvement in sidewall surface roughness of the fabricated waveguides for the optimal combination of parameters relative to nonoptimized parameters. The following sections describe the specific experimental procedures and the outcomes.

2. Experimental Procedure

The optical waveguides were fabricated on silicon wafers with SiO_2 used as a material for bottom cladding and polysilicon as a core material. Approximately 1 μm of SiO_2 was grown on two in wafers in an atmospheric furnace at 1050°C. Next, 1.2 μm of polysilicon was grown in a low-pressure furnace at 600°C. AZ4620 photoresist was spin coated using Laurel Spinner. After spinning, the wafer was soft baked in the nitrogen furnace for 40 min at 90°C and rehydrated in the atmosphere for 1 h before the photolithography was done on a Quintil Q-2001C mask aligner. Then, the wafer was diced and etching experiments were conducted on dies from the same wafer to minimize variations between experiments.

The photoresist structure was first characterized using a HITACHI S-70 scanning electron microscope (SEM) and low surface roughness has been demonstrated. Initial silicon etching experiments were conducted at a power of 100 W and pressure of 100 mTorr, with varying ratios of SF_6 and O_2 gas mixtures for optimization of the etch rate [19]. Then, a set of experiments with different combinations of pressure and power were conducted in a parallel plate capacitively coupled 13.56 MHz RF Plasma Therm plasma reactor (Table 1).

There were 15 types of experiments for each combination of pressure and power. The total flow rate of the gases was kept constant at 50 SCCM for all of the experiments.

The fabricated waveguides were characterized using a SEM and the sidewalls' roughness values were then estimated from the images. The optimal parameters determined based on outcomes of all of the experiments were 30 mTorr and 150 W for pressure and RF power, respectively. Then, a two-inch wafer with SiO_2 cladding and a polysilicon core layer was processed under optimal conditions. After that, the wafer was cleaved and transmission losses of the fabricated waveguide were measured using the cutback method [20].

Table 1. Experimental Design for Optimizing the Dry Etching Recipe for Smooth Waveguide Walls

Pressure (mTorr)	RF Power (W)		
15	100	150	200
30	100	150	200
50	100	150	200
100	100	150	200

3. Results and Discussion

According to [21,22], the radiation losses of a waveguide are proportional to the square of the sidewall roughness. Therefore, the goal of our study was to minimize the roughness as much as possible with the capacitively coupled plasma reactor setup taking into consideration that a 125 nm roughness is the upper limit for the reasonable quality waveguide [10]. In order to optimize surface roughness on the nanometer scale all of the fabrication steps were characterized using a SEM. After the deposition of layers of SiO_2 and polysilicon, the photoresist was spin coated and patterned. Figure 1 shows a scanning electron micrograph of the photoresist line cross section with a width of 4.3 μm and smooth walls.

Then, in order to optimize etching parameters, the first step was to find optimal gas chemistry. While SF_6 to O_2 are gases used in traditional Si etching recipes [19,23], further characterization was needed to understand the influence of gas flow ratios on the etch rate and selectivity of the photoresist. Figure 2(a) demonstrates the etch rate of the polysilicon versus the flow ratio of SF_6 to O_2. The maximum rates are observed for SF_6 concentrations between 80% and 90%. The low etch rates for lower concentrations of SF_6 can be attributed to the lower effective temperature of electrons in the plasma, while at higher concentrations it can be due to the lowering of electron density [24,25], both of which influence the degree of ionization in the plasma chamber and the etching of polysilicon. At the same time, the presence of oxygen can also be important for the improvement of the etching efficiency by removing the polymer products formed during etching.

Another important parameter of the etching process that needs to be monitored for photoresist integrity is the selectivity of the etching of the photoresist versus polysilicon. Figure 2(b) shows selectivity as a function of oxygen concentration in plasma and in the flow. While 100% SF_6 yields the maximum selectivity, it corresponds to a very slow etch rate due to the depletion of oxygen; therefore, 90% concentration was used based on a trade-off between selectivity and the etch rate.

The next step was to choose a set of parameters for further optimization. Recently, fabrication processes

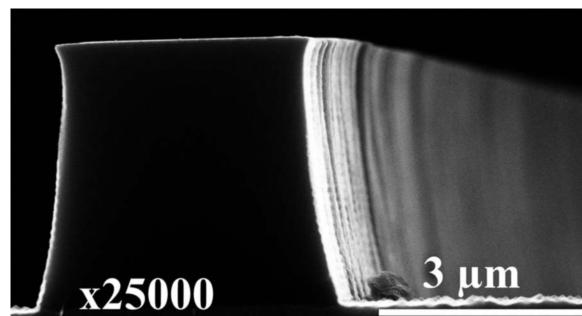

Fig. 1. Scanning electron micrograph of an AZ4620 photoresist waveguide pattern taken after photolithography and before the etching.

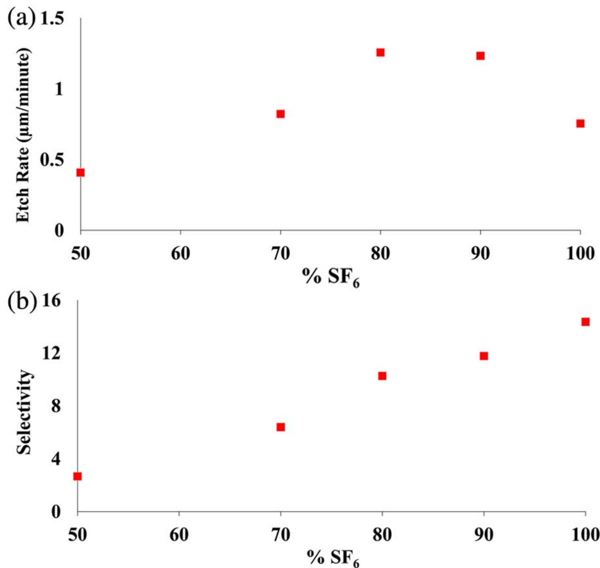

Fig. 2. (a) Etch rate of polysilicon versus the ratio of SF_6–O_2 and (b) selectivity of the etching of polysilicon versus the photoresist conducted at 100 mTorr pressure, 100 W power, and 50 SCCM of the total flow of gases.

using capacitively coupled plasma reactors have been studied [25–30], and the main parameters used in optimization were pressure, power, and their combination. The experimental design of optimization based on these two parameters is presented in Table 1. The pressure was varied from 15 to 100 mTorr for three RF plasma powers (100, 150, and 200 W) and the corresponding surface roughness was estimated using a SEM [16,31]. All of the waveguides were imaged under identical conditions (Fig. 3). The height variation (Z_{ij}) was determined from the SEM images at 9 different points of each waveguide. The estimations were taken at identical locations across all samples in areas of the image where it was focused best. The roughness approximations were done at 3 different heights and 3 different displacements along the waveguide in a 3×3 square grid labeled Z_{ij}, where $i = 1$ to 3 was changing along the waveguide and $j = 1$ to 3 across the waveguide.

The estimated roughness values were calculated using Eq. (1) ($m = n = 3$) and the summary of these results is plotted in Fig. 4,

$$\mathrm{RMS} = \sqrt{\frac{1}{m * n} \sum_{i=1}^{m} \sum_{j=1}^{n} Z_{ij}^2}. \quad (1)$$

Further analysis demonstrates that for 100 W power (Fig. 3-I) and pressure range 15–100 mTorr [(a), (b), (c), and (d)], at lower pressures the smoothness of the sidewalls is improved and at higher pressures the walls are more vertical. The estimated roughness is reduced from 71 to 35 nm, as the pressure is decreased from 100 to 15 mTorr (Fig. 4). Figure 3-II demonstrates the SEM images for higher power (150 W) and the same pressure ranges 15–100 mTorr [(a), (b), (c), and (d)]. The roughness decreases as the pressure is reduced. However, it can be noted that for 100 mTorr the sidewalls for 150 W are smoother (estimated roughness of 45 nm) than for 100 W RF (71 nm roughness). This may be due to the increase in the etch rate, plasma density, ionization, and dissociation of species at high powers [16].

For the power of 200 W, a decrease in surface roughness was also observed when the pressure was reduced from 100 to 15 mTorr [Fig. 3-III (a), (b), (c), and (d)]. However, for the pressure 100 mTorr, the surface roughness slightly increased (59 nm) in comparison with the value at 150 W (45 nm) due to higher acceleration of species in the plasma reactor.

To summarize, it can be seen from the sidewall roughness summary in Fig. 4 that for the capacitively coupled plasma reactors the optimal combination of the pressure and the power that gives the lowest surface roughness can be determined. For the constant power level, higher pressures increased roughness of the sidewalls. This can be explained by the fact that high pressure would block the products of etching from escaping. Decrease in pressure at a constant power increases the mean free path of reactive species in the plasma [32], thus producing

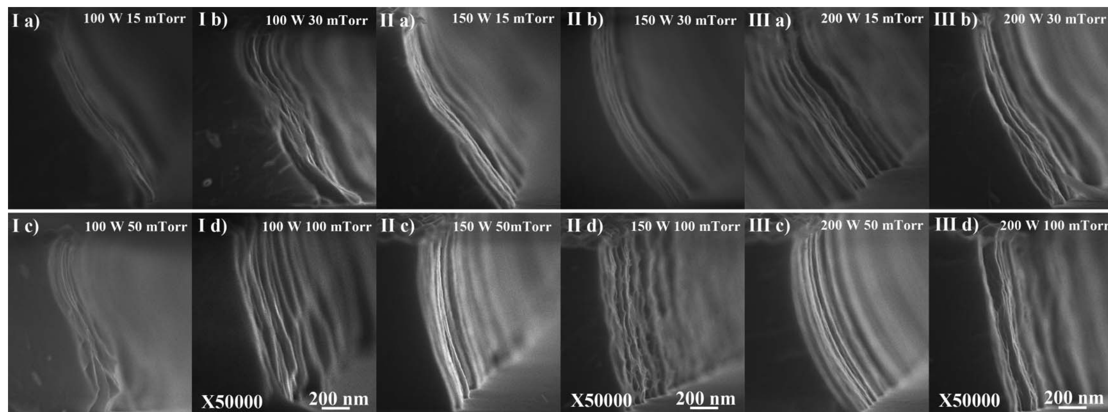

Fig. 3. Scanning electron micrographs of waveguides etched using experimental designs presented in Table 1. (I), (II), and (III) correspond to 100, 150, and 200 W power, respectively, and labels (a), (b), (c), and (d) are shown for pressures 15, 30, 50, and 100 mTorr.

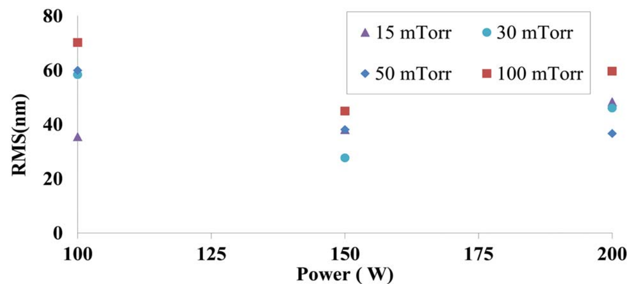

Fig. 4. Plots of root mean square roughness (RMS) versus the power of the etch at all pressures in the experiment.

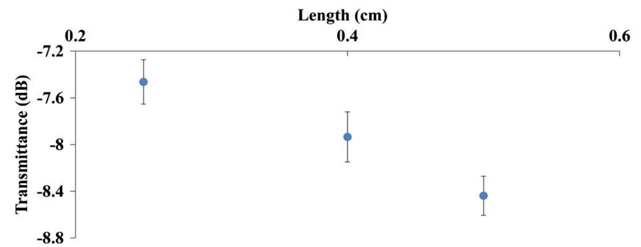

Fig. 5. Measured attenuation of light (dB) after propagation in waveguides of three different lengths.

smoother sidewalls. However, further decrease to a much lower pressure, 15 mTorr, results in increased roughness possibly caused by enhanced ion bombardment [4]. In all of the experiments with varying power, the pressures higher than 50 mTorr resulted in rougher surfaces. The optimal combination of the pressure and power for the reactor setup was determined to be 30 mTorr and 150 W, with the estimated roughness value of 27 nm. The nonoptimized parameters resulted in surface roughness as high as 71 nm, thus proper optimization provides us with a 62% improvement.

After determining the optimal parameters, the next step was to calculate the transmission losses of the fabricated waveguide and compare with the losses for polysilicon waveguides fabricated using ICP reactive ion etching.

The measurements were done for the wavelength of 1550 nm, which has very low absorption loss in silicon. The overall absorption loss is influenced by the dimensions of a waveguide [1,33,34]. For example, a loss of 6.2 dB/cm was reported for a polysilicon waveguide width of 120 nm [35] and just 0.56 dB/cm was reported for a 10 μm width waveguide [36]. Since the width of our waveguide is 3.6 μm, the high quality waveguide should have a loss between those two values.

The losses of the waveguide fabricated using optimized conditions of our reactor, 150 W and 30 mTorr, were studied using the cutback method [20]. All of the waveguides were fabricated with the same width of 3.6 μm. Then, they were cleaved at 3 different lengths, L_1, L_2, and L_3. Coupling of light into the waveguide was done from an optical fiber using a high precision XYZ stage while observing it under a microscope. The output mode was monitored to insure that the measurement was conducted for light properly coupled into the waveguide. The transmitted output power was measured directly by a power meter. For each length, six measurements of the transmitted power were conducted. Additionally, direct measurement of light without any waveguides was used to determine the base power. Powers measured for each length, L_1, L_2, and L_3, were averaged to P_1, P_2, and P_3, respectively, and transmission loss coefficients were calculated for three sets of lengths, $(L_1 - L_2)$, $(L_2–L_3)$, $(L_1–L_3)$ using Eq. (2) from [1], where m, n are 1, 2, or 3. Finally, an average of those three values was 4.1 dB/cm with a standard error of ±0.6 dB/cm. Figure 5 demonstrates transmission losses of T_1, T_2, and T_3 (in dB) corresponding to the averaged powers of P_1, P_2, and P_3 for 3 waveguide lengths.

$$a_{mn}\left(\frac{\mathrm{dB}}{\mathrm{cm}}\right) = \left(\frac{10}{L_m - L_n}\right)\log\left(\frac{P_m}{P_n}\right) = \left(\frac{T_m - T_n}{L_m - L_n}\right). \quad (2)$$

4. Conclusion

Here, we demonstrated the application of a capacitively coupled plasma reactor for the fabrication of polysilicon optical waveguides with smooth sidewalls and described several levels of the optimization of multiple fabrication parameters. First, the influence of the flow ratio of SF_6 to O_2 gases was studied and the optimal ratio was found to be 90%/10%. Next, the optimal combination of the pressure and power was determined to be 30 mTorr and 150 W, with a very low estimated surface roughness value of 27 nm. Additionally, the fabricated waveguides have a low propagation loss of 4.1 ± 0.6 dB/cm. This demonstration of the use of a capacitively coupled plasma reactor for polysilicon waveguide fabrication would potentially enable the use of silicon photonics in a larger number of universities possessing this equipment.

We wish to thank the USF Nanotechnology Research & Education Center and its staff members for their great help and high professionalism.

References

1. L. Liao, D. R. Lim, A. M. Agarwal, X. Duan, K. K. Lee, and L. C. Kimerling, "Optical transmission losses in polycrystalline silicon strip waveguides: effects of waveguide dimensions, thermal treatment, hydrogen passivation, and wavelength," J. Electron. Mater. **29**, 1380–1386 (2000).
2. A. Säynätjoki, S. Arpiainen, J. Ahopelto, and H. Lipsanen, "High-index-contrast optical waveguides on silicon," in *Physics of Semiconductors: 27th International Conference on the Physics of Semiconductors–ICPS 27* (2005), pp. 1537–1538.
3. A. Yimit, A. G. Rossberg, T. Amemiya, and K. Itoh, "Thin film composite optical waveguides for sensor applications: a review," Talanta **65**, 1102–1109 (2005).
4. E. Jaberansary, T. M. B. Masaud, M. M. Milosevic, M. Nedeljkovic, G. Z. Mashanovich, and H. M. H. Chong, "Scattering loss estimation using 2-D Fourier analysis and modeling of sidewall roughness on optical waveguides," IEEE Photon. J. **5**, 6601010 (2013).

5. T. Barwicz and H. A. Haus, "Three-dimensional analysis of scattering losses due to sidewall roughness, in microphotonic waveguides," J. Lightwave Technol. **23**, 2719–2732 (2005).
6. S. V. Kartalopoulos, *Introduction to DWDM Technology: Data in a Rainbow* (Wiley, 2000).
7. K. K. Lee, D. R. Lim, L. C. Kimerling, J. Shin, and F. Cerrina, "Fabrication of ultralow-loss Si/SiO_2 waveguides by roughness reduction," Opt. Lett. **26**, 1888–1890 (2001).
8. F. Ladouceur, J. D. Love, and T. J. Senden, "Effect of side wall roughness in buried channel waveguides," IEE Proc. Optoelectron. **141**, 242–248 (1994).
9. Z. Zhou, "Accurate top-down processing of silicon photonic devices," J. Micro-nanolithogr. SPIE Newsroom, 2010, http://spie.org/x38925.xml?highlight=x2402&ArticleID=x38925.
10. D. K. Sparacin, K. Wada, and L. C. Kimerling, "Oxidation kinetics of waveguide roughness minimization in silicon microphotonics," in *Integrated Photonics Research Conference* (Optical Society of America, 2003), paper ITuC4.
11. D. K. Sparacin, S. J. Spector, and L. C. Kimerling, "Silicon waveguide sidewall smoothing by wet chemical oxidation," J. Lightwave Technol. **23**, 2455–2461 (2005).
12. J. N. Cai, P. H. Lim, Y. Ishikawa, and K. Wada, "Silicon waveguide sidewall smoothing by resist reflowing," J. Nonlinear Opt. Phys. Mater. **19**, 801–809 (2010).
13. S. Jette-Charbonneau, N. Lahoud, R. Charbonneau, G. Mattiussi, and P. Berini, "End-facet polishing of surface plasmon waveguides in lithium niobate," IEEE Trans. Adv. Packag. **31**, 479–483 (2008).
14. S. C. Hung, E. Z. Liang, and C. F. Lin, "Silicon waveguide sidewall smoothing by KrF excimer laser reformation," J. Lightwave Technol. **27**, 887–892 (2009).
15. K. Solehmainen, T. Aalto, J. Dekker, M. Kapulainen, M. Harjanne, K. Kukli, P. i. Heimala, K. Kolari, and M. Leskel, "Dry-etched silicon-on-insulator waveguides with low propagation and fiber-coupling losses," J. Lightwave Technol. **23**, 3875–3880 (2005).
16. W. Li, Y. Ruan, B. Luther-Davies, A. Rode, and R. Boswell, "Dry-etch of As_2S_3 thin films for optical waveguide fabrication," J. Vac. Sci. Technol. A **23**, 1626–1632 (2005).
17. W. T. Li, D. A. P. Bulla, J. Love, B. Luther-Davies, C. Charles, and R. Boswell, "Deep dry-etch of silica in a helicon plasma etcher for optical waveguide fabrication," J. Vac. Sci. Technol. A **23**, 146–150 (2005).
18. V. M. Donnelly and A. Kornblit, "Plasma etching: yesterday, today, and tomorrow," J. Vac. Sci. Technol. A **31**, 050825 (2013).
19. R. d'Agostino and D. L. Flamm, "Plasma etching of Si and SiO_2 in SF_6–O_2 mixtures," J. Appl. Phys. **52**, 162–167 (1981).
20. J. Schmidtchen, A. Splett, B. Schuppert, K. Petermann, and G. Burbach, "Low loss singlemode optical waveguides with large cross-section in silicon-on-insulator," Electron. Lett. **27**, 1486–1488 (1991).
21. F. P. Payne and J. P. R. Lacey, "A theoretical analysis of scattering loss from planar optical waveguides," Opt. Quantum Electron. **26**, 977–986 (1994).
22. P. K. Tien, "Light waves in thin films and integrated optics," Appl. Opt. **10**, 2395–2413 (1971).
23. R. Legtenberg, H. Jansen, M. de Boer, and M. Elwenspoek, "Anisotropic reactive ion etching of silicon using $SF_6/O_2/CHF_3$ gas mixtures," J. Electrochem. Soc. **142**, 2020–2028 (1995).
24. R. S. Pessoa, L. L. Tezani, H. S. Maciel, G. Petraconi, and M. Massi, "Study of SF_6 and SF_6/O_2 plasmas in a hollow cathode reactive ion etching reactor using Langmuir probe and optical emission spectroscopy techniques," Plasma Sources Sci. Technol. **19**, 025013 (2010).
25. S. Kechkar, P. Swift, J. Conway, M. Turner, and S. Daniels, "Investigation of atomic oxygen density in a capacitively coupled O_2/SF_6 discharge using two-photon absorption laser-induced fluorescence spectroscopy and a Langmuir probe," Plasma Sources Sci. Technol. **22**, 045013 (2013).
26. Q. Z. Zhang, Y. X. Liu, W. Jiang, A. Bogaerts, and Y. N. Wang, "Heating mechanism in direct current superposed single-frequency and dual-frequency capacitively coupled plasmas," Plasma Sources Sci. Technol. **22**, 025014 (2013).
27. F. Hamaoka, T. Yagisawa, and T. Makabe, "Numerical investigation of relationship between micro-scale pattern, interfacial plasma structure and feature profile during deep-Si etching in two-frequency capacitively coupled plasmas in SF_6/O_2," J. Phys. D **42**, 075201 (2009).
28. A. Watanabe, F. Ishikawa, and M. Kondow, "Effects of plasma processes on the characteristics of optical device structures based on GaAs," Jpn. J. Appl. Phys. **51**, 056501 (2012).
29. T. Ray, H. Zhu, and D. R. Meldrum, "Deep reactive ion etching of fused silica using a single-coated soft mask layer for bio-analytical applications," J. Micromech. Microeng. **20**, 097002 (2010).
30. Y. Miyawaki, Y. Kondo, M. Sekine, K. Ishikawa, T. Hayashi, K. Takeda, H. Kondo, A. Yamazaki, A. Ito, H. Matsumoto, and M. Hori, "Highly selective etching of SiO_2 over Si_3N_4 and Si in capacitively coupled plasma employing C_5HF_7 gas," Jpn. J. Appl. Phys. **52**, 016201 (2013).
31. G. A. Porkolab, P. Apiratikul, B. Wang, S. H. Guo, and C. J. K. Richardson, "Low propagation loss AlGaAs waveguides fabricated with plasma-assisted photoresist reflow," Opt. Express **22**, 7733–7743 (2014).
32. M. Ohring, *Materials Science of Thin Films* (Academic, 2001), p. 818.
33. T. M. Ben Masaud, A. Tarazona, E. Jaberansary, X. Chen, G. T. Reed, G. Z. Mashanovich, and H. M. H. Chong, "Hot-wire polysilicon waveguides with low deposition temperature," Opt. Lett. **38**, 4030–4032 (2013).
34. A. M. Agarwal, L. Liao, J. S. Foresi, M. R. Black, X. M. Duan, and L. C. Kimerling, "Low-loss polycrystalline silicon waveguides for silicon photonics," J. Appl. Phys. **80**, 6120–6123 (1996).
35. J. S. Orcutt, S. D. Tang, S. Kramer, K. Mehta, H. Q. Li, V. Stojanovic, and R. J. Ram, "Low-loss polysilicon waveguides fabricated in an emulated high-volume electronics process," Opt. Express **20**, 7243–7254 (2012).
36. D. Kwong, J. Covey, A. Hosseini, Y. Zhang, X. C. Xu, and R. T. Chen, "Ultralow-loss polycrystalline silicon waveguides and high uniformity 1 × 12 MMI fanout for 3D photonic integration," Opt. Express **20**, 21722–21728 (2012).